International Journal of Theoretical Physics (2025) 64:69
https://doi.org/10.1007/s10773-025-05930-w

RESEARCH

The Influence of Global Monopole Space-time on Bound States, Scattering States and Thermodynamic Functions with Manning-Rosen Potential

H. I. Alrebdi[1] · A. N. Ikot[2,3] · U. S. Okorie[4] · R. Horchani[5] · G. J. Rampho[4]

Received: 8 January 2025 / Accepted: 20 February 2025

Abstract

In this study, the analytical eigensolutions of the radial Schrödinger equation with a point-like global monopole under the combined Manning-Rosen potential and screened Coulomb self-interaction potential has been investigated. The Greene-Aldrich approximation was used to overcome the centrifugal barrier which allows for the derivation of the energy and wave function in closed form. The solution of the energy and wave function were applied to investigate the scattering phase shift and thermodynamics function variations with topological defect parameter, quantum numbers and temperature, respectively. The results reveal that the energy eigenvalues and wave function amplitudes are influenced by the quantum numbers and the topological defect parameters. The shift in energy eigenvalues observed are caused by the particle collisions that exist in the system. The scattering phase shifts were found to be sensitive to the rotational quantum numbers and topological defect values. The thermodynamic plots exhibit high dependency on the temperature and topological defect parameters considered. Specific observation is the Schottky anomaly which exists uniquely for the topological defect values at low temperatures. Our results agree with occurrences in physical phenomenon, as recorded in literatures.

✉ U. S. Okorie
okoriu@unisa.ac.za

H. I. Alrebdi
hialrebdi@pnu.edu.sa

A. N. Ikot
ndemikotphysics@gmail.com

R. Horchani
horchani@squ.edu.om

G. J. Rampho
ramphjg@unisa.ac.za

1 Department of Physics, College of Science, Princess Nourah bint Abdulrahman University, P.O. Box 84428, Riyadh 11671, Saudi Arabia

2 Theoretical Physics Group, Department of Physics, University of Port Harcourt, Port Harcourt, Rivers State, Nigeria

3 Western Caspian University, Baku, Azerbaijan

4 Department of Physics, University of South Africa, Florida, 1710 Johannesburg, South Africa

5 Department of Physics, College of Science, Sultan Qaboos University, P.O. Box 36, P. C. 123, Al-Khod Muscat, Sultanate of Oman

Published online: 04 March 2025

Keywords Bound state · Scattering state · Thermodynamic functions · Global monopole · Manning-Rosen potential · Screened Coulomb-like potential

1 Introduction

The task for every theoretical Physicist is to obtain the solutions of exactly solvable models in quantum mechanics. These solutions of exactly solvable models in quantum mechanics are very few and such are only those of harmonic oscillators and hydrogen atom. Subsequently, many physical systems cannot be solved exactly, therefore many researchers adopt different approximate techniques to obtain its solutions [1–9]. Once the solutions of the Schrödinger equation (SE) are obtained one can extract useful and necessary information out of it such as thermal properties and entropic information. Apart from the well-known Minkowski space-time which many quanta theory of physics was formulated, many attempts have been made by different researchers in investigating the SE in the presence of curvature and torsion in the space-time. The implication of SE in a curved space-time leads to the concepts of topological defects [10–16]. The topological defects are generally observed in condensed and gravitation physics. In gravitation physics, the concepts of topological defects were observed in the evolution of the early universe where symmetry breaking phase transition occurs [17, 18] while topological defects were observed in material synthesis in condensed matter physics [19, 20]. Claudio and Moraes [21] studied the bound states of electrons and holes to disclinations within the framework of the theory of defects. It was observed that positive disclinations repelled both electrons and holes, while negative disclinations attracted the electrons and holes, thereby increasing the bound states. Bakke et al. [22] investigated the non-relativistic quantum dynamics of induced electric dipoles with topological defects, by employing Landau quantization for neutral atoms. Their results show that the topological defect was responsible for the breaking of the infinite degeneracy of Landau levels.

The impact of various topological defects on thermal, magnetic and optical properties with some potential models have been investigated in recent times [23–32]. Permatahati et al. [33] showed that the topological defect and magnetic field can cause a shift and modification in the energy spectrum, partition function, absorption coefficient and refractive index of the DMs. The screened modified Kratzer potential was employed to study the confinement effects of the AB flux and magnetic fields with topological defect on carbon monoxide molecule [34]. The results in this study were seen to exhibit paramagnetic and diamagnetic tendencies for weak and strong magnetic fields, respectively. Other studies involving the topological defects in relativistic regimes can been seen in Refs. [35–43].

In recent times, the studies of the scattering state phase shift of selected confining potential models have attracted much attention, in relation to topological defects [44]. Furtado et al. [45] investigated the quantum scattering problem of one electron by a screw dislocation by using the Katanaev-Volovich theory of defects in solids. In their studies, the scattering amplitude was seen to be of the Aharonov-Bohm type and the Berry's phase was observed in the dynamics of the electron with the screw dislocation. Recently, Alves et al. [46] studied the influence of electron by the Hulthén potential in a space-time containing a topological defect. Approximate solution for the scattering phase shift and the s-matrix were obtained for the Hulthén problem, in addition to the bound state solutions. Most recently, the Kratzer and screened modified Kratzer potentials have been studied in a global monopole space-time [47]. It was discovered that the topological defect has some notable influence on their effective potentials and energy spectra.

A particular potential model of interest in this study is the Manning-Rosen potential (MRP) model [48]. This molecular potential has received a wider attention over the decades in the areas of atomic and molecular physics to model atomic interactions in diatomic molecules and to analyze rotational and vibrational energy levels [49–53], in thermodynamics [54, 55], in nuclear physics to study bound states in quarkonium systems [56–58] and hadronic interactions [59, 60]. This is because it has been used as a bridge between theoretical exploration and practical applications in these areas of study. In plasma science, the MRP has been modelled to describe screening effect of weakly coupled plasma on H-atom [61]. With the help of Jost function, Behara [61] obtained eigen solutions of MRP, which were used to study absorption oscillator strengths, transition probabilities and dipole polarization of H-atom.

In this work, we will first solve the SE to obtain the bound state energy, subject to the combination of the MRP and a screened Coulomb-like self-interaction potential in the presence of a point-like global monopole (PGM). Also, the normalized wave function of the combined potential is obtained in terms of Jacobi polynomials. Thereafter, the scattering phase shift solutions of the combined potentials with PGM will be obtained, together with its normalization constant. In addition, the partition function and other thermodynamic functions of the combined potentials are obtained. graphical results of the bound state energy, scattering phase shift and thermodynamic functions at topological parameters and quantum states are discussed. Our motivation is pivoted on the fact that there is no report on the effect of topological defect on bound state energy spectra, scattering phase shift and thermodynamic functions of MRP with screened Coulomb self-interaction potential, to the best of our knowledge.

2 Non-Relativistic Quantum Theory in the Global Monopole Space-Time

In this section, the quantum theory of bound and scattering state energies in the non-relativistic regime of MRP and a screened Coulomb-like self-interaction potential in the presence of a point-like global monopole (PGM) will be determined.

2.1 Bound States

In $(3+1)$ dimensional space-time, the line element of the global monopole space-time is given by $(c=1)$

$$ds^2 = -dt^2 + \frac{dr^2}{\alpha^2} + r^2 d\theta^2 + r^2 \sin^2\theta d\varphi^2 \tag{1}$$

where $0 < \alpha^2 < 1$, $\alpha^2 = 1 - 8\pi G\eta_0^2$ and it characterize the topological deficit solid of the manifold of the system, G is the universal Newton's gravitational constant and the parameter η_0^2 is associated to the scale of gauge symmetry [62].

The three-dimensional SE in spherical coordinate reads

$$-\frac{\hbar^2}{2M}\nabla^2\psi(r,\theta,\varphi) + V(r)\psi(r,\theta,\varphi) = E\psi(r,\theta,\varphi) \tag{2}$$

where M is the mass of the particles, E is the energy, is the reduced Planck constant, ∇^2 is the Laplacian operator and $V(r)$ is the potential interaction being the sum of the Manning-Rosen potential and the electrostatic self-interaction potential given as

$$V(r) = V_{MR}(r) + V_{SI}(r) \tag{3}$$

Where $V_{MR}(r)$ represent the Manning-Rosen potential and $V_{SI}(r)$ is the electrostatic self-interaction potential. The electrostatic self-interaction potential $V_{SI}(r)$ has been defined in literature as a Coulomb-like potential of the form [44],

$$V_{SI}(r) = \frac{K(\alpha)}{r} \tag{4}$$

where r corresponds to the distance from the electron to the monopole and $K(\alpha)$ represents the coupling constant. In this work, we proposed a more generalized self- interaction potential in the form of screened Coulomb-like potential of the form,

$$V_{SI}(r) = \frac{K(\alpha)e^{-\eta r}}{r} \tag{5}$$

where $\eta = \delta^{-1}$ is the screening parameter and reduced to self-interaction Coulomb-like potential when $\eta \to 0$. The coupling constant characterized the behaviour of the potential and depending on its sign the potential can either be repulsive or attractive. The coupling constant $K(\alpha)$ is defined as [46],

$$K(\alpha) = \frac{e^2 S(\alpha)}{2} > 0 \tag{6}$$

where e is the electronic charge and the function $S(\alpha)$ is defined as [46],

$$S(\alpha) = \sum_{l=0}^{\infty} \left[\frac{2l+1}{\sqrt{4l(l+1)+\alpha^2}} - 1 \right] \tag{7}$$

Here, the global monopole dependent function $S(\alpha)$ is positive for $\alpha < 1$, negative when $\alpha > 1$ and l is the orbital angular momentum quantum number. l is a finite parameter which depends on the global monopole and screening parameter. The Manning-Rosen potential $V_{MR}(r)$ of (3) takes the form [48],

$$V_{MR}(r) = \frac{\eta^2}{k} \left[\frac{Ae^{-2\eta r}}{(1-e^{-\eta r})^2} - \frac{Be^{-\eta r}}{(1-e^{-\eta r})} \right] \tag{8}$$

where A and B are the potential parameters, k is an arbitrary constant and η is the screening parameter.To find the solution to (2), we proceed by taking an ansatz for the wave function of the form $\psi_{nlm}(r,\theta,\varphi) = F_{nl}(r)Y_{lm}(\theta,\varphi)$, where $F_{nl}(r)$ is the radial eigen-function and $Y_{lm}(\theta,\varphi)$ is the eigen-function of the angular part called the spherical harmonics. Substituting the above ansatz function into (2) yields the following three second order differential equations:

$$-\frac{\hbar^2\alpha^2}{2Mr^2}\frac{\partial}{\partial r}\left(r^2\frac{\partial}{\partial r}\right)F_{nl}(r) - (E - V(r))F_{nl}(r) = -\frac{\hbar^2\alpha^2 l(l+1)}{2M}F_{nl}(r) \tag{9}$$

$$L^2 Y_{lm}(\theta,\varphi) = \hbar^2 l(l+1)Y_{lm}(\theta,\varphi) \tag{10}$$

$$L_z Y_{lm}(\theta,\varphi) = \hbar m Y_{lm}(\theta,\varphi) \tag{11}$$

where $m = -l, 0, +l$ and the z-component of the angular momentum L_z operator and the angular momentum square L^2 operator are given as,

$$L_z = -i\hbar\frac{\partial}{\partial\varphi} \tag{12}$$

$$L^2 = -\hbar^2\left(\frac{\partial^2}{\partial\theta^2} + \cot\theta\frac{\partial}{\partial\theta} + \frac{1}{\sin^2\theta}\frac{\partial^2}{\partial\varphi^2}\right) \tag{13}$$

To solve the radial part of the SE of (9), we assume the wave function $F_{nl}(r) = r^{-1}R_{nl}(r)$. This becomes

$$-\frac{\hbar^2\alpha^2}{2M}\frac{d^2R_{nl}(r)}{dr^2} + [E - V_{eff}(r)]R_{nl}(r) = 0 \tag{14}$$

where $V_{eff}(r)$ is the effective potential defined as,

$$V_{eff}(r) = \frac{\hbar^2\alpha^2}{2M}\frac{l(l+1)}{r^2} + \frac{K(\alpha)e^{-\eta r}}{r} + \frac{\eta^2}{k}\left[\frac{Ae^{-2\eta r}}{(1-e^{-\eta r})^2} - \frac{Be^{-\eta r}}{(1-e^{-\eta r})}\right] \tag{15}$$

Substituting (15) into (14) and after simplification, we obtain

$$\frac{d^2R_{nl}(r)}{dr^2} + \left[\begin{array}{c} \frac{2ME}{\hbar^2\alpha^2} - \frac{l(l+1)}{\alpha^2r^2} - \frac{2MK(\alpha)e^{-\eta r}}{\hbar^2\alpha^2 r} \\ \\ -\frac{2M\eta^2}{\hbar^2\alpha^2 k}\left(\frac{Ae^{-2\eta r}}{(1-e^{-\eta r})^2} - \frac{Be^{-\eta r}}{(1-e^{-\eta r})}\right) \end{array}\right] R_{nl}(r) = 0 \tag{16}$$

Up to date, there is no analytical solution that exits for the solutions of the type of (16) as shown in many available literatures. However, different approximation techniques for the centrifugal term $l(l+1)r^{-2}$ have been explored by many authors in providing an approximation solution to such equation. To find the solutions to (16), we invoke the Greene-Aldrich approximation scheme for the centrifugal term of the forms [63–66]

$$\left.\begin{array}{c} \frac{1}{r^2} \approx \frac{\eta^2}{(1-e^{-\eta r})^2}; \frac{1}{r} \approx \frac{\eta}{(1-e^{-\eta r})}; \\ \frac{1}{r^2} \approx \frac{\eta^2 e^{-2\eta r}}{(1-e^{-\eta r})^2} \end{array}\right] \tag{17}$$

By inserting (17) into (16) in view of the new coordinate transformation, $z = e^{-\eta r}$ with the boundary conditions $z \to 0$ as $r \to \infty$ and $z \to 1$ as $r \to 0$, and (16) becomes,

$$z^2\frac{d^2R_{nl}(z)}{dz^2} + z\frac{dR_{nl}(z)}{dz} + \left[\begin{array}{c} \frac{2ME}{\hbar^2\alpha^2\eta^2} - \left(\frac{l(l+1)}{\alpha^2} + \frac{2MA}{\hbar^2\alpha^2 k}\right)\frac{z^2}{(1-z)^2} \\ \\ +\left(\frac{2MB}{\hbar^2\alpha^2 k} - \frac{2MK(\alpha)}{\hbar^2\alpha^2\eta}\right)\frac{z}{(1-z)} \end{array}\right] R_{nl}(z) = 0 \tag{18}$$

A closer inspection of (18) show that it has singularities at $z = 0$ and $z = 1$. Therefore, the wave function of (18) can be written in the form,

$$R_{nl}(z) = z^{\mu}(1-z)^{v}H_{nl}(z) \tag{19}$$

where,

$$\mu = \sqrt{-\frac{2ME}{\hbar^2\alpha^2\eta^2}}; v = \frac{1+\sqrt{1+4\gamma}}{2}; \gamma = \frac{l(l+1)}{\alpha^2} + \frac{2MA}{\hbar^2\alpha^2 k} \tag{20}$$

Substituting (19) into (18) yields a second-order differential equation of the hypergeometric-type of the form,

$$\begin{aligned} &z(1-z)H_{nl}^{''}(z)+[1+2\mu-(1+2\mu+2v)z]\,H_{nl}^{'}(z)\\ &-\left(\mu+v+\sqrt{\mu^2+\gamma+\Lambda}\right)\left(\mu+v-\sqrt{\mu^2+\gamma+\Lambda}\right)H_{nl}(z)=0 \end{aligned} \tag{21}$$

where,

$$\Lambda=\frac{2MB}{\hbar^2\alpha^2k}-\frac{2MK(\alpha)}{\hbar^2\alpha^2\eta} \tag{22}$$

We can see that (21) is the hypergeometric equation of the form [68],

$$y(1-y)H_{nl}^{''}(y)+[c-(1+a+b)]\,H_{nl}^{'}(y)-(ab)H_{nl}(y)=0 \tag{23}$$

Comparing (21) and (23), we obtain the constants a, b, c as follows,

$$a=\left(\mu+v+\sqrt{\mu^2+\gamma+\Lambda}\right);b=\left(\mu+v-\sqrt{\mu^2+\gamma+\Lambda}\right);c=(1+2\mu)\Big] \tag{24}$$

Whenever a or b equal to the negative integer, the hypergeometric function $H_{nl}(z)$ turns to a polynomial of degree n. Here, $n=0,1,2...n_{max}$, where n_{max} is the maximum vibrational quantum number. Therefore, the solution of (21) becomes,

$$H_{nl}(z)=\ {}_2F_1(a,b,c;z) \tag{25}$$

By using the quantization condition,

$$b=-n\Rightarrow\left(\mu+v-\sqrt{\mu^2+\gamma+\Lambda}\right)=-n \tag{26}$$

We obtain the energy spectra for the MRP with screened Coulomb-like self-interaction potential in the global monopole space-time as,

$$E_{nl}=-\frac{\hbar^2\alpha^2\eta^2}{2M}\left[\frac{\frac{l(l+1)}{\alpha^2}+\frac{2M(A+B)}{\hbar^2\alpha^2k}-\frac{2MK(\alpha)}{\hbar^2\alpha^2\eta}}{2(n+\Xi)}-\frac{(n+\Xi)}{2}\right]^2 \tag{27}$$

where,

$$\Xi=\frac{1}{2}\left(1+\sqrt{1+\frac{4l(l+1)}{\alpha^2}+\frac{8MA}{\hbar^2\alpha^2k}}\right) \tag{28}$$

It can be seen in (27) and (28) that the energy spectrum for the MRP with screened Coulomb-like self-interaction potential depends on the topological defect parameter. In the absence of the electrostatic self-interaction potential ($V_{SI}(r)=0$) and the topological defect parameter ($\alpha=0$), (27) reduces to the energy expression (15) in ref. [67].

The corresponding wave function can be obtained using (19) and (25) as,

$$R_{nl}(r)=N_{nl}\left(e^{-\eta r}\right)^{\mu}\left(1-e^{-\eta r}\right)^{v}\ {}_2F_1(a,b,c;z) \tag{29}$$

where N_{nl} is the normalization constant. In terms of Jacobi polynomials, we have

$$R_{nl}(r)=N_{nl}\left(e^{-\eta r}\right)^{\mu}\left(1-e^{-\eta r}\right)^{v}P_n^{(2\mu,2v-1)}\left(1-2e^{-\eta r}\right) \tag{30}$$

To obtain the normalization constant, the normalization condition of the radial wave function is employed:

$$\int_0^\infty |R_{nl}(r)|^2\, dr = 1 \tag{31}$$

Considering the condition at $r \in (0, \infty)$ and $e^{-\eta r} \in (0, 1)$, we have

$$-\frac{N_{nl}^2}{\eta}\int_1^0 z^{2\mu}(1-z)^{2v}\left[P_n^{(2\mu,2v-1)}(1-2z)\right]^2\frac{dz}{z} = 1, \left(z = e^{-\eta r}\right) \tag{32}$$

By using the transformation $Q = 1 - 2z$, we have the following boundary of (32) change from $z \in (1, 0)$ to $Q \in (-1, 1)$. This gives

$$\frac{N_{nl}^2}{2\eta}\int_{-1}^1 \left(\frac{1-Q}{2}\right)^{2\mu-1}\left(\frac{1+Q}{2}\right)^{2v}\left[P_n^{(2\mu,2v-1)}(Q)\right]^2 dQ = 1, \tag{33}$$

From the standard integral formula [69],

$$\begin{aligned}&\int_{-1}^1 \left(\frac{1-q}{2}\right)^{w}\left(\frac{1+q}{2}\right)^{y}\left[P_n^{(w,y-1)}(Q)\right]^2 dq\\ &= \frac{2^{w+y+1}\Gamma(1+n+w)\Gamma(1+n+y)}{n!\Gamma(1+n+w+y)\Gamma(1+2n+w+y)}\Bigg]\end{aligned} \tag{34}$$

By comparing (33) and (34), the normalization constant becomes

$$N_{nl} = \sqrt{\frac{2\eta(n!)\Gamma(n+2\mu+2v)\Gamma(2n+2\mu+2v)}{2^{2\mu+2v}\Gamma(n+2\mu)\Gamma(1+n+2v)}} \tag{35}$$

The normalized wave function for the Manning-Rosen potential with screened Coulomb-like self-interaction potential in the global monopole space-time now becomes

$$\begin{aligned}R_{nl}(r) = \sqrt{\frac{2\eta(n!)\Gamma(n+2\mu+2v)\Gamma(2n+2\mu+2v)}{2^{2\mu+2v}\Gamma(n+2\mu)\Gamma(1+n+2v)}}\left(e^{-\eta r}\right)^{\mu}\left(1-e^{-\eta r}\right)^{v}\\ P_n^{(2\mu,2v-1)}\left(1-2e^{-\eta r}\right)\end{aligned} \tag{36}$$

2.2 Scattering States

In this section, we proceed to study the scattering state Schrödinger equation within the global monopole space-time framework. By substituting (17) into (15) with a new coordinate transformation of the form $x = (1 - e^{-\eta r})$ and (16) becomes

$$x(1-x)\frac{d^2R_{nl}(x)}{dx^2} + x\frac{DR_{nl}(x)}{dx} + \left[\begin{array}{c}\frac{2ME}{\hbar^2\alpha^2\eta^2}\left(\frac{x}{1-x}\right) - \frac{(\frac{l(l+1)}{\alpha^2}+\frac{2MA}{\hbar^2\alpha^2 k})(1-x)}{x}\\ \\ -\frac{2M}{\hbar^2\alpha^2}\left(\frac{B}{K}-\frac{K(\alpha)}{\eta}\right)\end{array}\right]R_{nl}(x) = 0 \tag{37}$$

Equation (37) has regular singularities at $x = 0, 1$ and ∞. Therefore $R(x = 1) = 0$ as $r \to \infty$ and $R(x = 0) = 1$ as $r \to 0$. Thus, the wave function can be written in the form,

$$R_{nl}(x) = x^s(1-x)^{-it}U_{nl}(x) \tag{38}$$

where,

$$s = \frac{1}{2}\left(1 + \sqrt{1 + \frac{4l(l+1)}{\alpha^2} + \frac{8MA}{\hbar^2\alpha^2 k}}\right); t = \sqrt{\frac{2ME}{\hbar^2\alpha^2\eta^2}} \tag{39}$$

Substituting (38) into (37) gives the hypergeometric Gauss differential equation of the form

$$\left.\begin{aligned} x(1-x)U_{nl}^{''}(x) + [2s - (2s - 2it + 1)x]\, U_{nl}^{'}(x) \\ - \left(s - it + \sqrt{\chi}\right)\left(s - it - \sqrt{\chi}\right) U_{nl}(x) = 0 \end{aligned}\right] \tag{40}$$

where,

$$\chi = \frac{l(l+1)}{\alpha^2} + \frac{2M}{\hbar^2\alpha^2}\left[\frac{A+B}{k} - \frac{K(\alpha)}{\eta}\right] \tag{41}$$

The solution of (40) is the hypergeometric function given as

$$U_{nl}(x) = {}_2F_1\left(\omega_1, \omega_2, \omega_3; x\right) \tag{42}$$

where,

$$\omega_1 = \left(s - it + \sqrt{\chi}\right); \omega_2 = \left(s - it - \sqrt{\chi}\right); \omega_3 = 2s \tag{43}$$

By using (38) and (42), we obtain the scattering wave function as

$$R_{nl}(x) = x^s(1-x)^{-it}\, {}_2F_1\left(\omega_1, \omega_2, \omega_3; x\right) \tag{44}$$

To obtain to the scattering phase shift, we used the following asymptotic properties [70]. As $R_{nl}(x) \to 0, x \to 0$, (44) becomes

$$R_{nl}(x) \to 2\sin\left[tx + \zeta - \frac{l\pi}{2} + \frac{\pi(l+1)}{2}\right], x \to \infty \tag{45}$$

where ζ is the scattering phase shift. The phase shift can be obtained from (45) as follows (see details in Ref. [71] for derivation for phase shift factor)

$$\zeta_l = \frac{\pi(l+1)}{2} + \arg\Gamma(\omega_3 - \omega_1 - \omega_2) - \arg\Gamma(\omega_3 - \omega_1) - \arg\Gamma(\omega_3 - \omega_2) \tag{46}$$

By using (43), (46) can be written as,

$$\zeta_l = \frac{\pi(l+1)}{2} + \arg\Gamma(2it) - \arg\Gamma(s - it - \sqrt{\chi}) - \arg\Gamma(s - it + \sqrt{\chi}) \tag{47}$$

It should be noted that the energy eigenvalues expression of (27) can be retrieved from (47) by employing the scattering amplitude definition from the general theory of the partial-wave method. Readers can refer to Ref. [72]. and other references therein.

3 Thermodynamic Functions

In this section, we will investigate the thermodynamic properties for the Manning-Rosen potential with screened Coulomb-like self-interaction potential under the influence of global

monopole. The vibrational partition function of any system at a given temperature T is defined to be [73]

$$Z(\beta) = \sum_{0}^{\sigma} e^{-\beta E_n}, \beta = \frac{1}{k_B T} \tag{48}$$

with σ being the maximumvibrational quantum number, k_B being the Boltzmann constant, T being the absolute temperature and E_n is the energy of the nth bound state. Putting (27) into (48) gives,

$$Z(\beta) = \sum_{0}^{\sigma} e^{\frac{\hbar^2\alpha^2\eta^2\beta}{2M}\left[\frac{l(l+1)}{\alpha^2}+\frac{2M(A+B)}{\hbar^2\alpha^2 k}-\frac{2MK(\alpha)}{\hbar^2\alpha^2\eta}}{2(n+\Xi)}-\frac{(n+\Xi)}{2}\right]^2} \tag{49}$$

To evaluate the vibrational partition function of (49), we employ the Euler-Maclaurin sum defined as [74–77],

$$\sum_{0}^{\infty} F(n) = \frac{1}{2}F(0) + \int_{0}^{\infty} F(n)dn - \sum_{p=1}^{\infty} \frac{B_{2p}}{(2p)!} F^{2p-1}(0) \tag{50}$$

where B_{2p} are the Bernoulli numbers and $F^{2p-1}(n)$ is the derivative of order $(2p-1)$ of the function $F(n)$ with $B_2 = \frac{1}{6}$, $B_4 = -\frac{1}{30}$ and $B_6 = \frac{1}{42}$. By employing (50), the vibrational partition function becomes,

$$\begin{aligned} Z(\beta) = \left(\frac{1}{2\sqrt{-G_1\beta}}\right) e^{-\left[\frac{G_1\left(\Xi^4+G_2^2\right)\beta}{4\Xi^2}+\frac{1}{2}\sqrt{-G_1\beta}\sqrt{-G_1G_2^2\beta}\right]} \\ \sqrt{\pi}\left(\begin{array}{l} -Erf\left[\frac{1}{2}\Xi\sqrt{-G_1\beta}-\frac{-G_1G_2^2\beta}{2\Xi}\right]+Erf\left[\frac{-\sqrt{-G_1G_2^2\beta}+\sqrt{-G_1\beta}(\Xi+\sigma)^2}{2(\Xi+\sigma)}\right] \\ +e^{\sqrt{-G_1\beta}\sqrt{-G_1G_2^2\beta}}\left(\begin{array}{l} -Erf\left[\frac{\Xi^2\sqrt{-G_1\beta}+\sqrt{-G_1G_2^2\beta}}{2\Xi}\right] \\ +Erf\left[\frac{\sqrt{-G_1G_2^2\beta}+\sqrt{-G_1\beta}(\Xi+\sigma)^2}{2(\Xi+\sigma)}\right] \end{array}\right) \end{array}\right) - \left(\frac{G_1(G_2^2-\Xi^4)\beta}{24\Xi^3}\right) \end{aligned} \tag{51}$$

where,

$$\begin{aligned} G_1 = \frac{\hbar^2\alpha^2\eta^2}{2M}; G_2 = \left(\frac{l(l+1)}{\alpha^2}+\frac{2M(A+B)}{\hbar^2\alpha^2 k}-\frac{2MK(\alpha)}{\hbar^2\alpha^2\eta}\right); \\ \sigma = \sqrt{G_2}-\Xi \end{aligned} \tag{52}$$

With (51), other thermodynamic functions such as Helmholtz free energy $F(\beta)$, entropy $S(\beta)$, internal energy $U(\beta)$ and specific heat, $C_v(\beta)$ can be obtained from the vibrational partition function as follows:

$$\begin{aligned} F(\beta) = -\frac{1}{\beta}\ln Z(\beta); U(\beta) = -\frac{d\ln Z(\beta)}{d\beta}; \\ S(\beta) = \ln Z(\beta) - \beta\frac{d\ln Z(\beta)}{d\beta}; C_v(\beta) = \beta^2\frac{d^2\ln Z(\beta)}{d\beta^2} \end{aligned} \tag{53}$$

4 Results and Discussions

In this study,the various results of energies and thermodynamic quantities under the influence of PGM for MRP and a screened Coulomb-like self-interaction potential will be analyzed. We

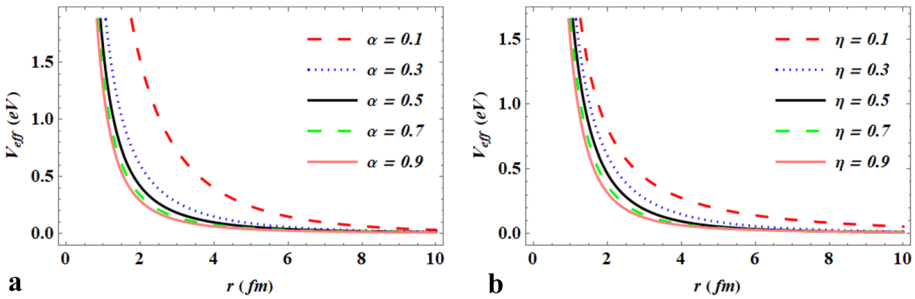

Fig. 1 Variation of screened Coulomb interaction potential with internuclear distance (r) for various values of (a) topological defect (α) (b) screening parameter (η)

first consider the variations the screened Coulomb self-interaction potential in (5), manning-Rosen potential in (8) and the effective potential in (15) with inter-nuclear distance, as shown in Figs. 1, 2 and 3, respectively. The screened Coulomb self-interaction potential in Fig. 1a and b decrease with increase in inter-nuclear distance for varying values of α and η. These curves tend to converge at higher values of r. This same trend is also observed for the effective potential in Fig. 3a and b. In Fig. 2, the MRP curves decrease and later gets deeper for higher values of η. As r is enhanced the more, the MRP curves converge at the origin.

The variation of the energy spectra of the Manning-Rosen potential and screened Coulomb-like self-interaction potential with different quantum numbers and topological defects is shown in Fig. 4. We see that the energy curves decrease as the quantum number increases, as shown in Fig. 4a and b. For any value of the quantum number, the energy increases with decrease in topological defect. In Fig. 4c, the energy increases sharply in a clustered form for principal quantum number considered at a particular value of α. As α increases, the energy curves diverge and thereafter remain constant for each value of n. In Fig. 4d, we observe a sharp increase in energy curves corresponding to l at unique values of α. As α is enhanced, the energy curves converge at a particular energy value.

The variation of squared wave function with inter-nuclear distance is presented in Fig. 5, for varying values of topological defect. We observe increase in the amplitude of the squared wave function plots, corresponding to a decrease in the values of topological defect. As the

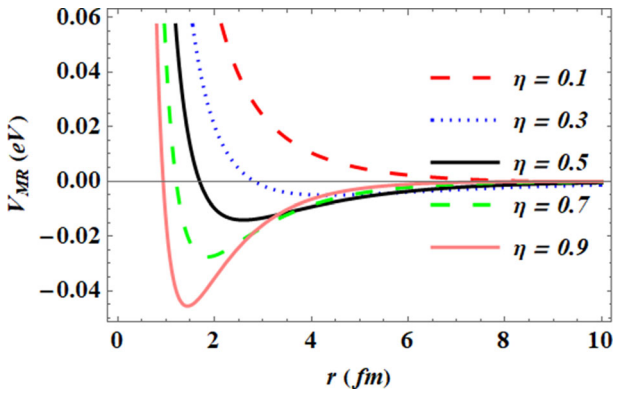

Fig. 2 Variation of Manning-Rosen potential with internuclear distance (r) for various values of screening parameter (η)

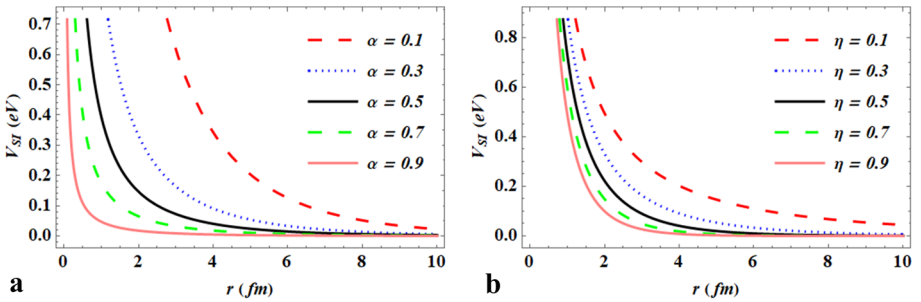

Fig. 3 Variation of effective potential with internuclear distance (r) for various values of (a) topological defect (α) (b) screening parameter (η)

quantum numbers increase, there is a tangible increase in the amplitude of the squared wave function, as seen in Fig. 5a, b, c, and d. This shows that the amplitude of the nodes and the number of nodes observed increase with increase in the number of excited states considered. It can be deduced here that the magnitude and electron concentration of particles considered rises with a reduction in the values of topological defect.

Figure 6 shows the variation of the scattering phase shift with orbital angular momentum quantum number, for various values of the topological defect. Here, we see a direct increase in the scattering phase shift corresponding to increase in l. Also, the scattering phase shift increases with decrease in topological defect, for a particular value of l.

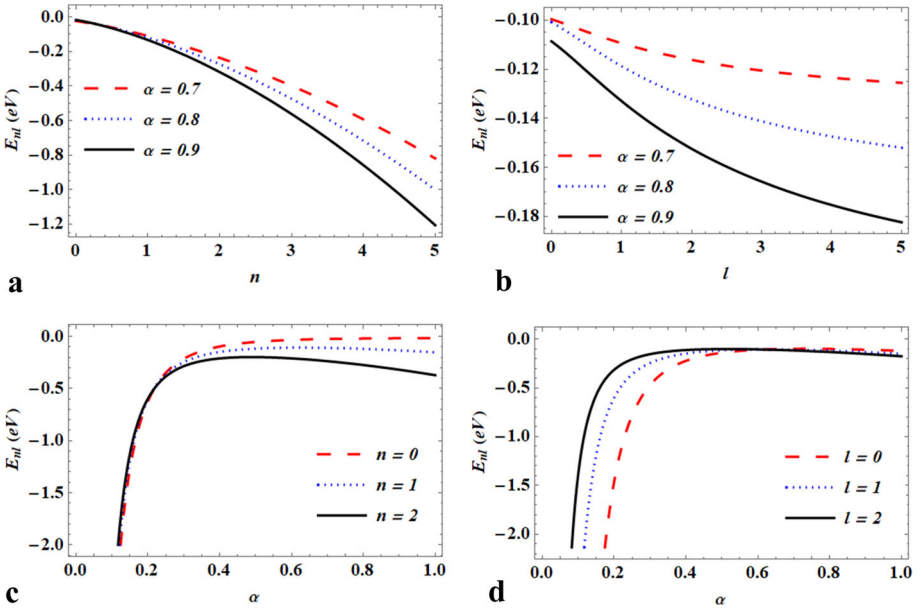

Fig. 4 Variation of Energy Spectra of the Manning-Rosen potential plus screened Coulomb-like self-interaction potential with (a) quantum numbers (n) for various topological defect (α); (b) quantum number (l) for various topological defect (α); (c) topological defect (α) for various quantum number (n); (d) topological defect (α) for various quantum number (l)

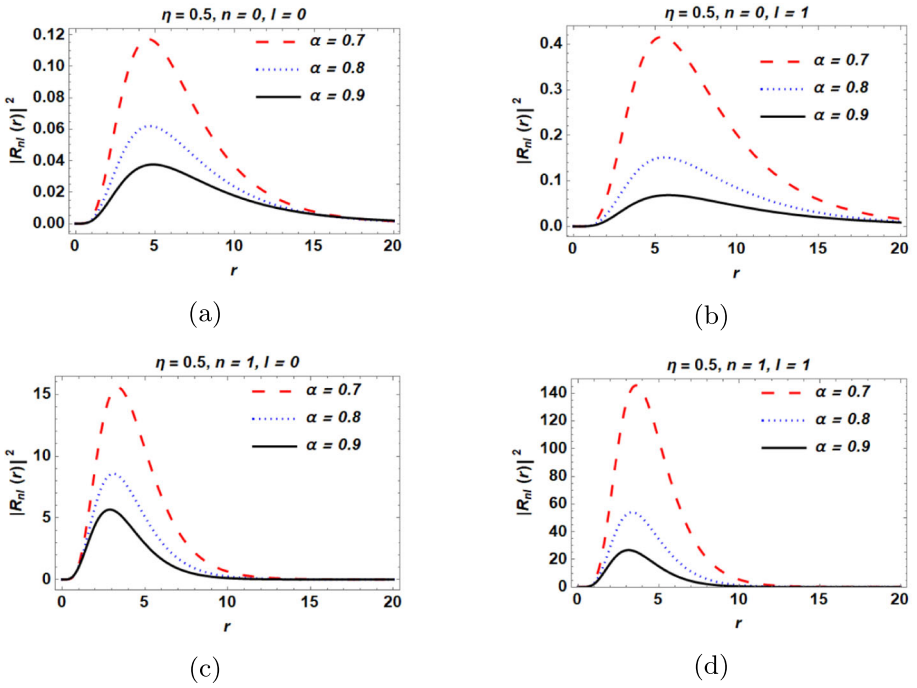

Fig. 5 Variation of squared wave function of the Manning-Rosen potential plus screened Coulomb-like self-interaction potential with internuclear distance (r) for various values of topological defect (α) with (a) $\alpha = 0.5$, $n = 0, l = 0$; (b) $\alpha = 0.5, n = 0, l = l$; (c) $\alpha = 0.5, n = 1, l = 0$; (d) $\alpha = 0.5, n = 1, l = 1$

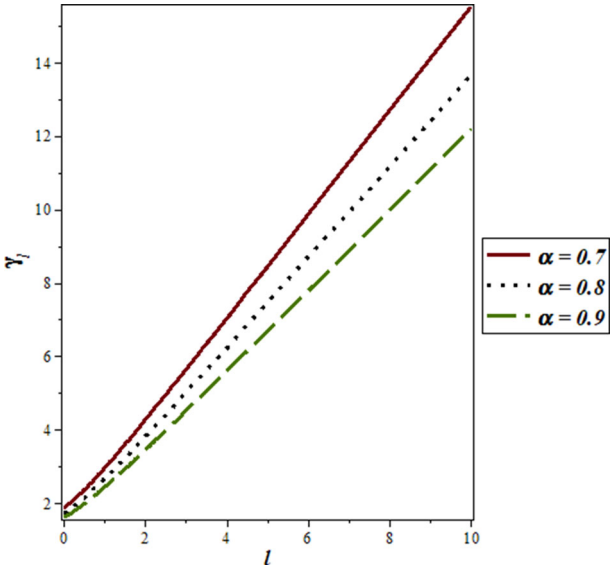

Fig. 6 Variation of scattering phase shift of the Manning-Rosen potential plus screened Coulomb-like self-interaction potential with quantum number (l) for various values of topological defect (α)

The plots of vibrational partition function and other thermodynamic functions with temperature for various topological defect values are presented in Fig. 7. In Fig. 7a, the vibrational partition function decreases sharply first at a zero temperature. As the temperature is increased, the vibrational partition function curves begin to increase with decrease in topological defect values considered. This indicates that more energies distributed in the system as the temperature is increased, with a decrease in topological defect values. The free energy curves are seen to decrease with increase in temperature, as shown in Fig. 7b. Also, the free energy decreases with decrease in topological defect values. This implies that the estimate of the useful work obtained in MRP plus screened Coulomb-like self-interaction potential decreases with increase in temperature and a decrease in topological defect parameters. In Fig. 7c and d, we observe that both the internal energy and entropy increase with increase in temperature. This increase occurs with a decrease in topological defect values considered. This shows that more molecular kinetic energies are generated as temperature rises, due to the molecular collisions that exist within the system. Hence, the occupation probability level

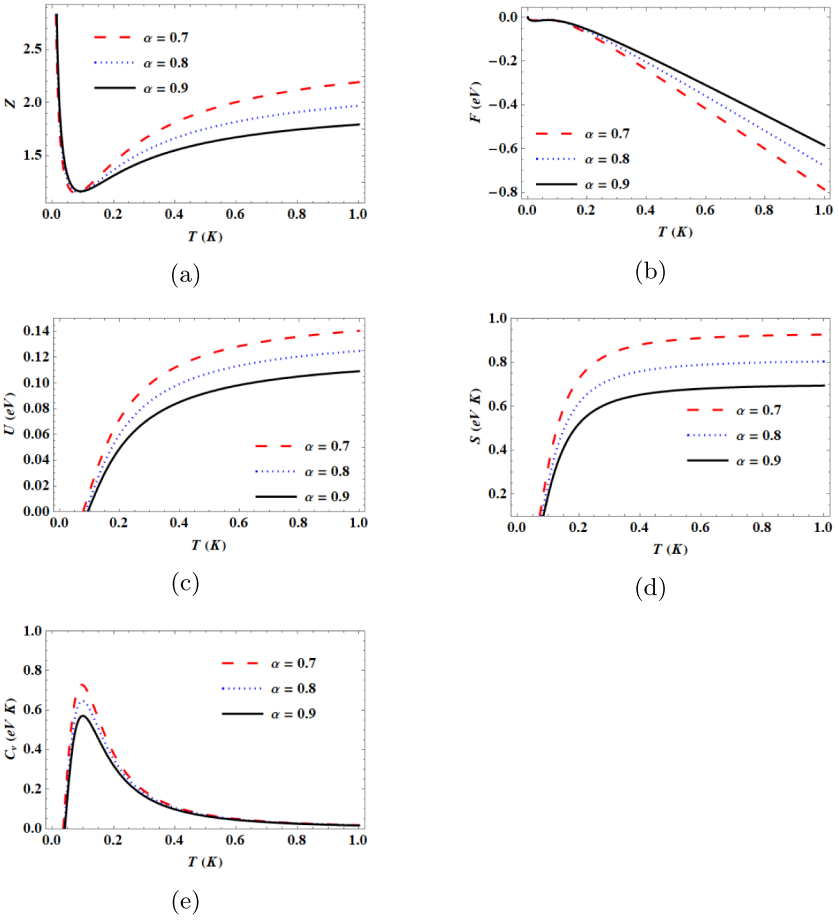

Fig. 7 Variation of (a) partition function; (b) free energy; (c) internal energy; (d) entropy and (e) specific heat capacity of the Manning-Rosen potential plus screened Coulomb-like self-interaction potential with temperature (T) for various values of topological defect (α)

of the kinetic energy of the system changes. Also, the increase in temperature causes the system's disorder to increase with decrease in topological defect values. Figure 7e shows a unique increase in specific heat capacity to peak values, corresponding to the values of topological defect considered at a particular temperature. As temperature is enhanced, the specific heat capacity curves decrease and thereafter converge at the origin as temperature values approaches 1K. This phenomenon points to the Schottky anomaly for lower temperatures ranges, corresponding to the topological defect values considered. This can be attributed to the probability of energy state distribution occupying the system under study [78]. In addition, the specific heat capacity values of this system obey the Dulong-Petit law for the values of the topological defect. This is a very significant phenomenon in condensed matter physics [79]. We can clearly see that the energy spectrum, wave function, scattering phase shift and thermodynamic functions exhibit meaningful variations in response to the topological defect changes, and this agrees to physical phenomena as recorded in literatures.

5 Conclusion

The eigensolutions of the non-relativistic radial Schrödinger equation with point-like global monopole with a combined MRP and screened Coulomb self-interaction potential has been obtained in this work. These solutions are obtained using the factorization method and the Greene-Aldrich approximation scheme, due to their effectiveness and simplicity in usage. These equations were applied to investigate the variation of the energy spectra, squared wave function, scattering phase shift and thermodynamic functions of the combined potentials with quantum numbers and the topological defect parameter. The squared wave functions amplitudes were found to increase with the increase in the topological defect parameters and quantum numbers. The scattering phase shifts were found to be sensitive to the rotational quantum number and topological defect parameter. In addition, the vibrational partition function and other thermodynamic functions considered are seen to vary with temperature and topological defect parameters.

Topological defects are seen to modify the particles of the combined MRP screened Coulomb self-interaction potential function, thereby influencing their energy levels and wavefunctions. This influence also causes a shift in the energy levels due to the topological change observed. Since the partition function depends on the energy levels of a MP potential, a shift in the energy eigenvalues due to the topological defect results in a shift in the partition function. This shift certainly results in the alteration of other thermodynamic functions. In addition, This change contributes to the alteration in the density of states of the system, thereby affecting the specific heat capacity of the system. Hence, topological defects has been seen to reshape the energy levels of MR potential by introducing different perturbations. These changes also affect the thermodynamic functions of the system. Its precise effect depends on the defect symmetry, dimensionality and interaction strength of the system under study. This study proves to be very significant in many areas of study due to its significant role in the understanding of the behaviour of particles in a global monopole space-time. Specific examples can be seen in refrigerating systems where molecular disorders are of necessity. Also, the Schottky anomaly can be very relevant in atomic and condensed matter physics, where magnetic behaviours are very relevant. It is our belief that this system can also be applied in the study of quantum dots and rings

Acknowledgements This work was supported by Princess Nourah bint Abdulrahman University Researchers Supporting Project number (PNURSP2025R106), Princess Nourah bint Abdulrahman University, Riyadh,

Saudi Arabia. Dr. U. S. Okorie acknowledges the support of the University of South Africa for the Postdoctoral Research Fellowship at the Department of Physics.

Author Contributions A. N. Ikot: Writing - original draft, Investigation, Formal analysis. U. S. Okorie: Writing - review & editing, Writing - original draft, Validation, Conceptualization. H. I. Alrebdi: Validation, Supervision, Project administration. R. Horchani: Methodology, Investigation, Formal analysis. G. J. Rampho: Writing - review & editing, Supervision.

Funding Open access funding provided by University of South Africa.

Data Availability No datasets were generated or analysed during the current study.

Declarations

Conflict of interest The authors declare no Conflict of interest.

References

1. Dong, S.H.: Factorization Method in Quantum Mechanics. Springer (2007)
2. Qiang, W.C., Dong, S.H.: EPL **89**, 10003 (2010)
3. Dong, S.H., Morales, D., Ravelo, J.G.: Int. J. Mod. Phys. E **16**, 189 (2007)
4. Gu, X.Y., Dong, S.H., Ma, Z.Q.: J. Phys. A: Math. Theor. **42**, 035303 (2009)
5. Falaye, B.J., Oyewumi, K.J., Ikhdair, S.M., Hamzavi, M.: Phys. Scr. **89**, 115204 (2014)
6. Nikiforov, A.F., Uvarov, V.B.: Special Functions of Mathematical Physics. Birkhauser, Basel (1988)
7. Ciftci, H., Hall, R.L., Saad, N.: Phys. Rev. A **72**, 022101 (2005)
8. Ciftci, H., Hall, R.L., Saad, N.: J. Phys. A: Math. Gen. **38**, 1147 (2005)
9. Ikot, A.N., Okorie, U.S., Amadi, P.O., Edet, C.O., Rampho, G.J., Sever, R.: Few-Body Syst. **62**, 9 (2021)
10. Hassanabadi, H., Zare, S., Kriz, J., Lutfuoglu, B.C.: EPL **132**, 60005 (2020)
11. Zare, S., Hassanabadi, H., de Montigny, M.: Int. J. Mod. Phys. A **35**, 2050071 (2020)
12. da Silva, W.C.F., Bakke, K.: Class. Quantum Grav. **36**, 235002 (2019)
13. Lutfuoglu, B.C., Kriz, J., Zare, S., Hassanabadi, H.: Phys. Scr. **96**, 015005 (2021)
14. Chen, H., Zare, S., Hassanabadi, H., Long, Z.W.: Ind. J. Phys. **96**, 4219 (2022)
15. Zare, S., Hassanabadi, H., Guvendi, A., Chung, W.S.: Int. J. Mod. Phys. A **37**, 2250033 (2022)
16. Alves, S.S., Cunha, M.M., Hassanabadi, H., Silva, E.O.: Universe **9**, 132 (2023)
17. Vilenkin, A.: Phys. Rep. **121**, 263–315 (1985)
18. Barriola, M., Vilenkin, A.: Phys. Rev. Lett. **63**, 341–343 (1989)
19. Kibble, T., Srivastava, A.: J. Phys. Cond. Matter **25**, 400301 (2013)
20. Bakke, K., Furtado, C., Sergeenkov, S.: Europhys. Lett. **87**, 30002 (2009)
21. Furtado, C., Moraes, F.: Phys. Lett. A **188**, 394 (1994)
22. Bakke, K., Ribeiro, L.R., Furtado, C.: Cent. Eur. J. Phys. **8**, 893 (2010)
23. Soheibi, N., Hamzavi, M., Eshghi, M., Ikhdair, S.M.: Eur. Phys. J. B **90**, 212 (2017)
24. Filgueiras, C., Rojas, M., Aciole, G., Silva, E.O.: Phys. Lett. A **379**, 2110 (2015)
25. Lambaga, R.D., Ramadhan, H.S.: Eur. Phys. J. C **78**, 436 (2018)
26. Boumali, A., Aounallah, H.: Rev. Mex. Fis. **66**, 192 (2020)
27. Braganca, E.A.F., Vitoria, R.L.L., Belich, H., Bezerra de Mello, E.R.: Eur. Phys. J. C **80**, 206 (2020)
28. Vitoria, R.L.L., Belich, H.: Phys. Scr. **94**, 125301 (2019)
29. Bakke, K., Furtado, C.: Int. J. Geo. Meth. Mod. Phys. **16**, 1950172 (2019)
30. Ikot, A.N., Okorie, U.S., Sawangtong, P., Horchani, H.: Int. J. Theor. Phys. **62**, 197 (2023)

31. Bouzeneda, A., Boumali, A., Serdouk, F.: Theor. Math. Phys. **216**(1), 1055–1067 (2023)
32. Nwabuzor, P., Edet, C.O., Ikot, A.N., Okorie, U.S., Ramantswana, M., Horchani, R., Abdel-Aty, A.H., Rampho, G.J.: Entropy **23**, 1060 (2021)
33. Permatahati, L.K., Cari, C., Suparmi, A., Harjana, H.: Int. J. Theor. Phys. **62**, 246 (2023)
34. Edet, C.O., Ikot, A.N.: J. Low Temp. Phys. **203**, 84–111 (2021)
35. Carvalho, J., Furtado, C., Moraes, F.: Phys. Rev. A **84**, 032109 (2011)
36. Bakke, K., Furtado, C.: Ann. Phys. **336**, 489 (2013)
37. Bakke, K.: Eur. Phys. J. Plus **127**, 82 (2012)
38. Bakke, K., Mota, H.: Eur. Phys. J. Plus **133**, 409 (2018)
39. Beuno, M.J., de Melo, J.L., Furtado, C., de M. Carvalho, A. M.: Eur. Phys. J. Plus **129**, 201 (2014)
40. Bakke, K., Furtado, C.: Phys. Lett. A **376**, 1269 (2012)
41. Vitoria, R.L.L., Furtado, C., Bakke, K.: Ann. Phys. **370**, 128 (2016)
42. Carvalho, J., de M. Carvalho, A.M., Cavalcante, E., Furtado, C.: Eur. Phys. J. C **76**, 365 (2016)
43. Neto, J.A., Bueno, M.J., Furtado, C.: Ann. Phys. **373**, 273 (2016)
44. Bezerra de Mello, E.R., Furtado, C.: Phys. Rev. D **56**(2), 1345 (1997)
45. Furtado, C., Bezerra, V.B., Moraes, F.: Europhys. Lett. **52**, 1 (2000)
46. Alves, S.S., Cunha, M.M., Hassanabadi, H., Silva, E.O.: Universe **9**, 132 (2023)
47. Alves, S.S., dos S. Azevedo, F., Filgueiras, C., Silva, E.O.: Chin. J. Phys. **88**, 609 (2024)
48. Eckart, C.: Phys. Rev. **35**, 1303 (1930)
49. Falaye, B.J., Oyewumi, K.J., Ibrahim, T.T., Punyasena, M.A., Onate, C.A.: Can. J. Phys. **91**, 98 (2013)
50. Nath, D., Roy, A.K.: Eur. Phys. J. Plus **136**, 430 (2021)
51. Ikhdair, S.M., Math, I.S.R.N.: Phys. **2012**, 201525 (2012)
52. Jia, C.S., Liang, G.C., Peng, X.L., Tang, H.M., Zhang, L.H.: Few-Body Syst. **55**, 1159 (2014)
53. Nasser, I., Abdelmonem, M.S., Abdel-Hady, A.: Mol. Phys. **111**, 1 (2013)
54. Louisa, H., Itab, B.I., Nzeata, N.I.: Eur. Phys. J. Plus **134**, 315 (2019)
55. Ghanbari, A., Khordad, R., Sharifzadeh, M.: Phys. B **678**, 415750 (2024)
56. Behera, A.K., Bhoi, J., Laha, U., Khirali, B.: Commun. Theor. Phys. **72**, 075301 (2020)
57. Khirali, B., Behera, A.K., Bhoi, J., Laha, U.: J. Phys. G: Nucl. Part. Phys. **46**, 115104 (2019)
58. Khirali, B., Behera, A.K., Bhoi, J., Laha, U.: Ann. Phys. **412**, 168044 (2020)
59. Sahoo, P., Laha, U.: Phys. Scr. **96**, 095302 (2021)
60. Swain, B., Laha, U., Behera, A.K.: Phys. Scr. **98**, 105308 (2023)
61. Behara, A.K.: Eur. Phys. J. Plus **139**, 804 (2024)
62. Bezerra de Mello, E.R.: Braz. J. Phys. **31**, 211 (2001)
63. Greene, R.L., Aldrich, C.: Phys. Rev. A **14**, 2363 (1976)
64. Nath, D., Roy, A.K.: Int. J. Quant. Chem. **121**, e26616 (2021)
65. Nath, D., Roy, A.K.: Chem. Phys. Lett. **780**, 138909 (2021)
66. Nath, D., Roy, A.K.: J. Math. Chem. **61**, 835 (2023)
67. Qiang, W.C., Dong, S.H.: Phys. Lett. A **368**, 13 (2007)
68. Dwork, B.: Generalized hypergeometric functions. Clarendon Press, Oxford (1990)
69. Gradshteyhn, I.S., Ryzhik, I.M.: Tables of integrals series and products, 7th edn. Academic Press, New York (2007)
70. Feng, W.G., Li, C.W., Ying, W.H., Yuan, L.Y.: Chin. Phys. B **18**, 3663 (2009)
71. Okorie, U. S., Ikot, A. N., Edet, C. O., Rampho, G. J., Horchani, R., Jelessi, H.: Eur, Phys. J. D. **75**, 53 (2021)
72. Wei, G.F., Liu, X.Y., Chen, W.L.: Int. J. Phys. **48**, 1649 (2009)
73. Ikot, A.N., Okorie, U.S., Onate, C.A., Onyeaju, M.C., Hassanabadi, H.: Can. J. Phys. **97**, 1161 (2019)
74. Boumali, A.: J. Math. Chem. **56**, 1656 (2018)
75. Arfken, G.: Mathematical methods for physicists, 3rd edn., pp. 327–338. Academic Press, Orlando (1985)
76. Chabi, K., Boumali, A.: Rev. Mex. Fis. **66**, 110 (2020)
77. Nath, D.: J. Math. Chem. **60**, 1819 (2022)
78. Khordad, R., Sedehi, H.R.R.: J. Low Temp. Phys. **190**, 200 (2017)
79. Servatkhah, M., Khordad, R., Firoozi, A., Sedehi, H.R.R., Mohammadi, A.: Eur. Phys. J. B **93**, 111 (2020)